

# On Numerical Simulation of Conductor Galloping Using Vortex Element Method

Olga A. Ivanova  
ivanovaolgaal@mail.ru

## Abstract

The algorithm for the transmission line conductor dynamics simulation using Galerkin method is developed. Some test computations are performed. It was shown that the mode of conductor galloping depends on the wind speed. The adequacy of the assumption about aerodynamic loads quasi-steadiness is discussed. The algorithm of the unsteady aeroelastic conductor motion simulation using vortex element method is proposed.

## 1 Introduction

A stable wind can cause galloping — high-amplitude low-frequency oscillations of overhead transmission lines. Galloping causes high dynamic loads which may damage overhead line, therefore a number of studies are dedicated to numerical and experimental modeling of the conductor dynamics (e.g., [1, 2, 3, 4]). The most wide-spread numerical method of the conductor dynamics simulation is the finite element method but the finite difference method and Galerkin method are also used.

The important part of the conductor dynamics simulation is aerodynamic loads computation. The generally accepted approach is that aerodynamic loads are proportional to the square of the relative wind speed and to the preliminarily determined stationary aerodynamic drag, lift and moment coefficients. It hasn't been investigated yet if this assumption about the quasi-steadiness of aerodynamic loads is always adequate. Though in many cases the agreement between numerical and experimental results is good, it is not clear how the real unsteadiness of the aerodynamic forces influences the conductor motion. But as the conductor has a large spatial extent, the full three-dimensional numerical simulation of its aeroelastic interaction with wind is hardly possible.

In this work a simplified approach to the direct numerical simulation of the unsteady aeroelastic conductor motion is proposed. The flat cross-section method is adopted, i.e. the aerodynamic loads are calculated in  $N$  separate conductor cross-sections under the assumption that the flow around them is plane-parallel. Thus a three-dimensional problem is replaced by a set of  $N$  partially independent two-dimensional problems of the flow simulation around the conductor's cross-sections. The computer parallel algorithm based on MPI technology usage which implements this approach is developed.

## 2 Mathematical model

### 2.1 Governing equations for the conductor dynamics

Let us locate the Cartesian coordinate system so that in the equilibrium position without aerodynamic loads the transmission line is located in the plane  $Ox_1x_3$ . The conductor is considered to be absolutely flexible and linearly elastic. Then its motion equations are the following [5]:

$$\begin{aligned} \frac{\partial}{\partial \xi} \left( \frac{Q}{1+Q/\alpha} \frac{\partial x_i}{\partial \xi} \right) + C_i + (1+Q/\alpha) q_i^a - \delta_{i3} - \frac{\partial^2 x_i}{\partial \tau^2} &= 0, \quad i = 1, 2, 3, \\ \left( \frac{\partial x_1}{\partial \xi} \right)^2 + \left( \frac{\partial x_2}{\partial \xi} \right)^2 + \left( \frac{\partial x_3}{\partial \xi} \right)^2 &= (1+Q/\alpha)^2, \\ \frac{\partial^2 \theta_m}{\partial \xi^2} + C_\theta + M^a - G_m \frac{\partial^2 \theta_m}{\partial \tau^2} &= 0. \end{aligned} \quad (1)$$

Here dimensionless parameters are:  $\xi \in [-0.5, 0.5]$  – natural coordinate on the unstretched conductor,  $\tau$  – time;  $Q(\xi, \tau)$  – tension;  $x_i(\xi, \tau)$ ,  $i = 1, 2, 3$  – cartesian coordinates of the conductor;  $\theta_m$  – the twist angle of conductor rotation without the change of its axis geometry;  $C_i(\partial x_i/\partial \tau)$ ,  $C_\theta(\partial \theta_m/\partial \tau)$  – internal damping forces;  $q_k^a(\xi, \tau)$ ,  $k = 1, 2, 3$ ,  $M^a$  – aerodynamic loads;  $\alpha = \text{const}$  – axial stiffness;  $G_m$  – torsional stiffness;  $\delta_{ij}$  – Kronecker delta. Initial condition is the equilibrium position in the gravity field  $x_{i0}(\xi)$ ,  $i = 1, 2, 3$ ,  $Q_0(\xi)$ ,  $\theta_{m0}(\xi)$ .

If the multispans line is considered the system similar to (1) describes the conductor motion in each span. Let us assume that at the equilibrium all insulators are vertical.

Different variants of boundary conditions at each end are possible (let us give them for the left end,  $\xi = -0.5$ ):

- Dead-end boundary conditions

$$\begin{aligned} x_1(-0.5, \tau) = x_{10}(-0.5), \quad x_2(-0.5, \tau) = 0, \quad x_3(-0.5, \tau) = x_{30}(-0.5), \\ \theta_m(-0.5) = 0. \end{aligned}$$

- Simple support type boundary conditions

$$\begin{aligned} Pr_{x_1}(Q(-0.5, \tau) - Q_0(-0.5)) &= K_1(x_1(-0.5, \tau) - x_{10}(-0.5)), \\ Pr_{x_2}Q(-0.5, \tau) &= K_2x_2(-0.5, \tau), \\ x_3(-0.5, \tau) &= x_{30}(-0.5), \\ \theta_m(-0.5) &= 0, \end{aligned}$$

where  $K_1$  and  $K_2$  are the stiffnesses of the equivalent linear static springs in  $Ox_1$  and  $Ox_2$  directions which model the adjacent spans and insulators. This approach was introduced in [7] for the span and in [8] for the insulators. Though it can not describe the dynamic coupling between the adjacent spans it is widely used.

- nonlinear coupling conditions for two adjacent spans in the suspension point; the insulator string is considered to be a uniform rigid rod.

The angle of incidence is calculated as

$$\theta = \theta_0 - \left( \frac{d}{2} \dot{\theta}_0 + \dot{x}_3 \right) / V_\infty$$

where  $\theta_0 = \arctan \frac{x_2}{x_3} + \theta_m$ .

## 2.2 Governing equations for the flow

The viscous incompressible flow around the airfoil (conductor cross-section) is described by continuity equation

$$\nabla \cdot \underline{V} = 0$$

and Navier – Stokes equation

$$\frac{\partial \underline{V}}{\partial t} - \underline{V} \times \underline{\Omega} = -\nabla \left( p + \frac{V^2}{2} \right) + \frac{1}{\text{Re}} \nabla^2 \underline{V},$$

where dimensionless parameters are:  $\underline{V}(x_2, x_3, t)$  – fluid velocity,  $\underline{\Omega} = \Omega \underline{e}_1$  ( $\underline{e}_1$  is axis  $Ox_1$  unit vector) – vorticity,  $p(x_2, x_3, t)$  – pressure,  $\text{Re}$  – Reynolds number. Boundary condition on the airfoil contour is no-slip condition; on infinity all perturbations decay and the flow has uniform velocity  $\underline{V}_\infty$  and pressure  $p_\infty$ .

## 3 Numerical scheme

The conductor motion equations are solved using Galerkin method, so the conductor coordinates and tension are taken in the form

$$x_i(\xi, \tau) = \sum_{k=1}^{n_i} a_k^{(i)}(\tau) \varphi_k^{(i)}(\xi), \quad i = 1, 2, 3,$$

$$\theta_m(\xi, \tau) = \sum_{k=1}^{n_\theta} a_k^{(\theta)}(\tau) \varphi_k^{(\theta)}(\xi), \quad Q(\xi, \tau) = \sum_{k=1}^{n_Q} a_k^{(Q)}(\tau) \varphi_k^{(Q)}(\xi).$$

The basis functions for the coordinates are the eigenmodes of the conductor small free oscillations which are computed using the accelerated convergence method [9]. For the coordinate  $x_1$  the linear function is added to the basis to satisfy the initial condition. The basis functions for the tension  $Q$  and for the twist angle  $\theta_m$  are trigonometric.

The flow around each cross-section of the conductor is simulated using meshfree lagrangian vortex element method [10].

## 4 Numerical examples

### 4.1 Vortex element method

Vortex element method allows to perform computations effectively on various multiprocessor systems [6]. This method has the following advantages:

- it allows to calculate the aerodynamic loads with the engineering accuracy in a reasonable time;
- it allows to simulate the flow around the arbitrary airfoil;
- the simulations of the flow around stationary and moving airfoils require almost the same computational time;
- it allows to develop effective parallel implementation.

The test computation was performed. Vortex wake around the iced conductor cross-section is shown on fig. 1



Figure 1: Vortex wake around the iced conductor cross-section

## 4.2 Conductor dynamics

Several test computations were performed; aerodynamic loads were calculated using the stationary aerodynamic coefficients. The drag and lift coefficients  $C_D(\theta)$  and  $C_L(\theta)$  (fig. 2) were assumed to be

$$C_D(\theta) = 2 + 0.2 \cos \theta, \quad C_L(\theta) = -1.5 \sin(2(\theta - \pi)).$$

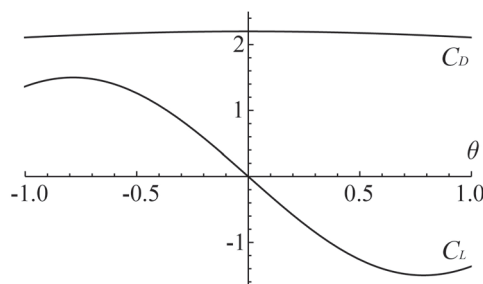


Figure 2: Aerodynamic loads dependencies on the angle of incidence

These dependencies  $C_D(\theta)$  and  $C_L(\theta)$  are close to the experimental data. Let us note that Den-Hartog instability criterion

$$C_D(\theta) + C_L'(\theta) < 0$$

is satisfied in the interval  $\theta \in (-0.37, 0.37)$ . The aerodynamic moment is not taken into account (for the conductor covered with thin icing the moment is close to zero).

The conductor dimensional parameters are those considered in [3]: axial rigidity  $29.7 \cdot 10^6$  N, horizontal component of tension  $32.0 \cdot 10^3$  N, diameter of the conductor  $28.6 \cdot 10^{-3}$  m, span length 243.8 m, mass per unit length 1.80 kg/m. The damping ratio in translational directions is 0.5 %. The sag-to-span ratio for these parameters is 0.0168.

In the test computations the wind velocity was varied from 5.7 to 11.4 m/s. The basis of Galerkin method contained 6 eigenmodes. Dead-end boundary conditions were applied. The computations were performed until the periodic response was achieved. In the table below the results are shown. The amplitudes refer to the point  $\xi = 0$  for single loop oscillation and to the point  $\xi = 0.25$  for two loop oscillation. The predominant galloping frequency is given in the fourth column.

The trajectories of the reference points in the plane  $Ox_2x_3$  are shown on fig. 3.

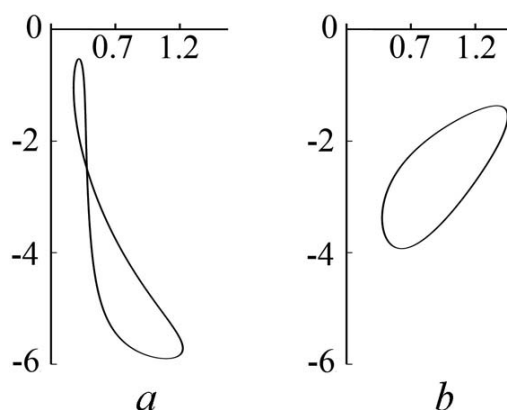
## 5 An algorithm of unsteady conductor dynamics analysis

The following parallel computer algorithm based on MPI technology usage is proposed to simulate the unsteady aeroelastic conductor motion (fig. 4).

| $V_\infty$ , m/s | Number of loops | Peak-peak galloping amplitude, m | $\omega$ , Hz |
|------------------|-----------------|----------------------------------|---------------|
| 5.7              | 1               | 4.40                             | 0.40          |
| 7.4              | 1               | 5.38                             | 0.38          |
| 8.0              | 1               | 5.40                             | 0.38          |
| 8.3              | 2               | 3.53                             | 0.57*         |
| 8.6              | 2               | 3.00                             | 0.57          |
| 9.1              | 2               | 2.94                             | 0.57          |
| 11.4             | 2               | 2.56                             | 0.54          |

\* – no clear periodic response was obtained

Table 13: The calculated characteristics of galloping


 Figure 3: *a* – the trajectory of the point  $\xi = 0$  at  $V_\infty = 7.4$  m/s, *b* – the trajectory of the point  $\xi = 0.25$  at  $V_\infty = 11.4$  m/s

1. Initialization; input data (the airfoil contour geometry etc.) loading.
2. All processes: 2D problem of the flow simulation during 1 time step; aerodynamic forces calculation.
3. Data exchange: all processes send calculated values of aerodynamic forces to the main process.
4. Main process: aerodynamic loads interpolation; the nonlinear ODE system obtained via Galerkin method solving during 1 time step.
5. Data exchange: main process broadcasts coefficients  $a_k^{(i)}$ ,  $a_k^{(\theta)}$ ,  $a_k^{(Q)}$  and their time derivatives to all processes.
6. All processes: airfoils new positions and angles calculation; return to p. 2.

The vortex element method requires that the bigger flow velocity is the smaller time step must be chosen. That is why the full aeroelastic simulation from the initial moment until the periodic response is extremely computationally costly. The simplified algorithm can be used: the periodic response can be found via the quasi-steady aerodynamic loads and then several galloping cycles with vortex element method are simulated and it is analyzed how it influences the limit cycle.

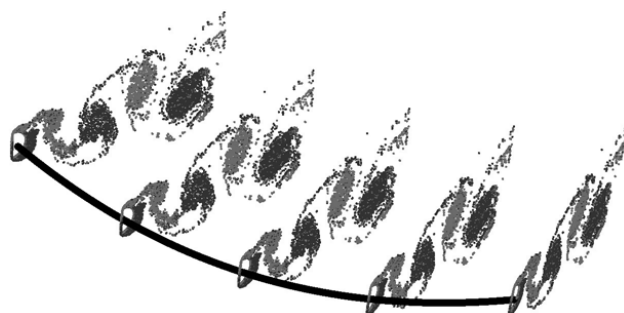


Figure 4: Flat cross-section method illustration

## 6 Conclusion

The program for the transmission line conductor dynamics simulation using Galerkin method is developed. The basis for Galerkin method contains the eigenmodes of the conductor small free oscillations. Several test computations were performed to investigate the influence of the wind speed on the characteristics of galloping. It is shown that with the increase of wind speed single loop galloping transforms to two loop one.

The problem of the adequacy of the assumption about aerodynamic loads quasi-steadiness hypothesis is discussed. The algorithm of the unsteady aeroelastic conductor motion simulation using vortex element method is proposed.

## Acknowledgements

The work was supported by Russian Federation Grant for young scientists [proj. MK-6482.2012.08]. The author thanks Joint Supercomputer Center of the Russian Academy of Sciences for the given possibility of supercomputer MVS-100k usage.

## References

- [1] O. Chabart, J.L. Lilien. Galloping of electrical lines in wind tunnel facilities // Journal of Wind Engineering and Industrial Aerodynamics. 1998. Vol. 74–76. P. 967–976.
- [2] Y.M. Desai, P. Yu, N. Popplewell, A.H. Shah. Finite Element Modelling Of Transmission Line Galloping // Computers and Structures. 1995. Vol. 57 (3). P. 407–420.
- [3] X. Wang, W.-J. Lou. Numerical approach to galloping of conductor // Proc. of the 7th Asia-Pacific Conference on Wind Engineering. Taipei, Taiwan, 2009.
- [4] L. Wang, J.-L. Lilien. Overhead Electrical Transmission Line Galloping // IEEE Trans. On Power Delivery. 1998. Vol. 13 (3). P. 909–916.
- [5] V.A. Svetlicky. Dynamics of rods. Springer, 2005.
- [6] V.S. Moreva, I.K. Marchevsky. High-Efficiency POLARA Program for Airfoil Aerodynamic Characteristics Calculation Using Vortex Elements Method // Proc. of the 5th International Conference on Vortex Flows and Vortex Models. San Leucio, Italy, 2010.
- [7] A.S. Veletsos, G.R. Darbre. Dynamic stiffness of parabolic cables // Int. J. Earthqu. Engng. Struct. Dyn. 1983. Vol. 11. P. 367–401.

- [8] R.K. Mathur, A.H. Shah, P.G.S. Trainor, N. Popplewell. Dynamics of a guyed transmission tower system // Trans. IEEE Power Deliv. 1987. PWRD-2 (3). P. 908–916.
- [9] L. Akulenko, S. Nesterov. High-precision methods in eigenvalue problems and their applications. Boca Raton: CRC Press, 2004.
- [10] G. Ya. Dynnikova. The Lagrangian approach to solving the time-dependent Navier-Stokes equations // Doklady Physics. 2004. Vol. 49 (11). P. 648–652.

*Olga A. Ivanova, Moscow, Russia*